13th IFAC/IFIP/IFORS/IEA Symposium on Analysis, Design, and Evaluation of Human-Machine Systems
Aug. 30 - Sept. 2, 2016. Kyoto, Japan

Effects of Preview Time on Human Control Behavior in Rate Tracking Tasks

K. van der El, S. Barendswaard, D.M. Pool and M. Mulder *

* *Faculty of Aerospace Engineering, Delft University of Technology, Delft, The Netherlands (email: [K.vanderEl], [S.Barendswaard], [D.M.Pool], [M.Mulder]@tudelft.nl).*

Abstract: In many practical control tasks, human controllers (HC) can preview the trajectory they must follow in the near future. This paper investigates the effects of the length of previewed target trajectory, or preview time, on HC behavior in rate tracking tasks. To do so, a human-in-the-loop experiment was performed, consisting of a combined target-tracking and disturbance-rejection task. Between conditions the preview time was varied between 0, 0.1, 0.25 0.5 0.75 or 1 s, capturing the complete human control-behavioral adaptation from zero- to full-preview tasks, where the performance remains constant. The measurements were analyzed by fitting a HC model for preview tracking tasks to the data. Results show that optimal performance is attained when the displayed preview time is higher than 0.5 s. When the preview time increases, subjects exhibit more phase lead in their target response dynamics. They respond to a single point on the target ahead when the preview time is below 0.5 s and generally to two different points when more preview is displayed. As the model tightly fits to the measurement data, its validity is extended to different preview times.

Keywords: Manual Control, Target Tracking, Preview, Parameter Estimation, Human Factors

1. INTRODUCTION

Much research has been conducted to increase our understanding of human manual control behavior since the 1960's. Despite great advancements for simple tasks, especially compensatory tracking (McRuer et al., 1965), the mechanisms underlying manual control behavior in more complex tasks with preview are still relatively unclear. Examples of such tasks include car driving, where the road ahead is visible through the windshield (Kondo and Ajimine, 1968), and flying an aircraft through a displayed tunnel-in-the-sky (Mulder and Mulder, 2005). In these tasks, a human controller (HC) can see and anticipate the future trajectory to follow, allowing for a more advanced control strategy that involves both feedforward and feedback (Sheridan, 1966; Ito and Ito, 1975; Van der El et al., 2015). Recently, Van der El et al. (2015) derived a new HC model for preview tracking with a physical foundation, enabling a more in-depth analysis on how humans exactly use preview information for control.

The effect of the previewed target trajectory's length (referred to as the preview time) on HC behavior has been abundantly studied (Reid and Drewell, 1972; Tomizuka and Whitney, 1973; Poulton, 1974; Ito and Ito, 1975; Van Lunteren, 1979). These authors report that HCs are able to track the target much better, and that the optimal performance in rate tracking tasks is already achieved with 0.5 s preview. The effect of additional preview beyond this so-called *critical preview time* is small, and tracking performance does not improve any further. However, using their new model, Van der El et al. (2015) found that HCs respond to a point on the target well *beyond* this critical preview time, in rate tracking tasks with 1 s of preview. It is unclear why HCs respond to the target further ahead when a similar performance is obtained with lower preview times.

The goal of this paper is to systematically analyze the effect of the displayed preview time on HC behavior in rate tracking tasks. To do so, we performed a human-in-the-loop experiment with integrator controlled element (CE) dynamics. Six conditions were tested, presenting 0, 0.1, 0.25, 0.5, 0.75 and 1 s of previewed target on the display, to capture the full human control-behavioral transition between situations without any preview to preview well beyond the reported critical preview time. First, the results are used to confirm previous findings that tracking performance improves with higher preview times. Then, the model from (Van der El et al., 2015) is fitted to the data to obtain the HC dynamics, including estimates of the points on the target responded to. These allow us to better explain how subjects use preview information. Finally, the Variance Accounted For (VAF) is calculated to confirm the model's validity in tasks with different preview times.

This paper is structured as follows. First, the new HC model for preview tracking is explained in Section 2, and an introduction to preview tracking is given. The parameter estimation method, used for fitting the model to the data, is explained in Section 3. Details of the experiment and its outcomes are presented in Sections 4 and 5. Finally, a discussion and our conclusions are presented in Sections 6 and 7.

2. BACKGROUND

2.1 Manual Preview Tracking

The preview display used for the considered preview tracking task is shown in Fig. 1. The amount of preview information of the target signal $f_t([t, t+\tau_p])$ that is visible ahead is characterized by the preview time τ_p. When τ_p equals zero, only the *current* target $f_t(t)$ is visible and the display reduces to what is referred to as a pursuit display (Wasicko et al., 1966).

The HC's task is to give control inputs $u(t)$ that drive the CE output $x(t)$ as close as possible to the current value of the target signal. In other words, subjects are to reduce tracking error, defined by $e(t) = f_t(t) - x(t)$. Only the lateral displacement of the CE is controlled; the previewed target signal moves down over the screen, so the current target also moves laterally. The CE (with dynamics $H_{ce}(j\omega)$) is additionally perturbed by a disturbance $f_d(t)$. Fig. 2 shows a schematic overview of the task.

2.2 Human Controller Model for Preview Tracking

Van der El et al. (2015) showed that HCs in preview tracking tasks can be modeled using a quasi-linear framework. This means that most of the HC's output is *linearly* related to the inputs. The remaining non-linearities and noise elements are modeled as filtered white noise (referred to as the remnant $n(t)$) added to the linear control output. The complete model is shown in Fig. 3.

The model's inner loop is similar to McRuer's simplified precision model for compensatory tracking task (McRuer et al., 1965). As such, the HC's structural adaptation to the CE dynamics is captured by $H_{o_{e^\star}}(j\omega)$, the *internal* error response, which is a pure gain $K_{e^\star}$ for an integrator CE:

$$H_{o_{e^\star}}(j\omega) = K_{e^\star}. \tag{1}$$

The inner loop further incorporates the human's physical limitations: τ_v represents the HC visual response time delay and H_{nms} the neuromuscular system dynamics. The latter are modeled as:

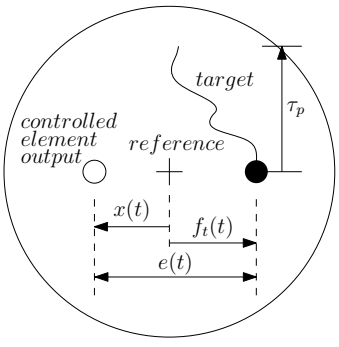

Fig. 1. Preview display.

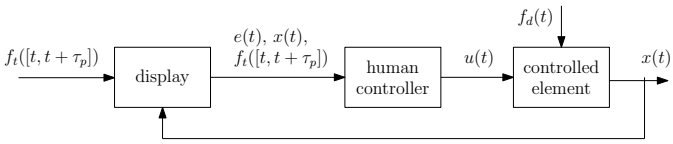

Fig. 2. Control task layout.

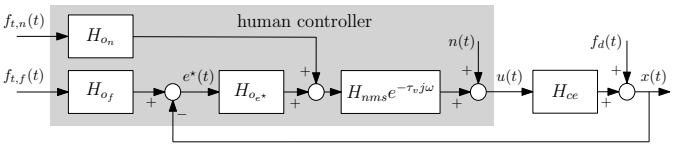

Fig. 3. Human controller model for preview tracking.

$$H_{nms}(j\omega) = \frac{\omega_{nms}^2}{(j\omega)^2 + 2\zeta_{nms}\omega_{nms}j\omega + \omega_{nms}^2}, \tag{2}$$

with natural frequency ω_{nms} and damping ratio ζ_{nms}.

For preview tracking tasks, the simplified precision model is extended with two responses with respect to different points on the previewed target. This near- and far-point ($f_{t,n}(t)$ and $f_{t,f}(t)$) are located τ_n and τ_f s ahead:

$$f_{t,n}(t) = f_t(t+\tau_n), \qquad f_{t,f}(t) = f_t(t+\tau_f). \tag{3}$$

By responding to the target ahead, HCs effectively introduce *negative* delays into the system, hence corresponding *phase lead*. This can be beneficial when used to compensate for their own response lags and the CE's inherent lag.

The far point is used to track to the slow changes (low frequencies) of the target signal. Its filtering dynamics $H_{o_f}(j\omega)$ thus has low-pass characteristics:

$$H_{o_f}(j\omega) = K_f \frac{1}{T_{l,f}j\omega + 1}, \tag{4}$$

with K_f and $T_{l,f}$ the far-point gain and lag time-constant, respectively. From the resulting filtered target signal HCs calculate the internal error $e^\star$, which in the frequency domain is given by

$$E^\star = H_{o_f}(j\omega)F_{t,f(j\omega)} - X(j\omega). \tag{5}$$

The capitals indicate the Fourier transforms of the respective signals.

The parallel near-point response $H_{o_n}(j\omega)$ was originally modeled as a high-pass filter. However, its estimated lag time-constant generally indicated a break frequency around 10 rad/s for tasks with integrator CE dynamics, which is in the region where the neuromuscular system dynamics also become dominant. Therefore, we omit the lag filter here, resulting in the following near-point response:

$$H_{o_n}(j\omega) = K_n j\omega, \tag{6}$$

with K_n the near-point gain.

Van der El et al. (2015) further showed that the model can be rewritten into an equivalent two-channel structure (see Fig. 4), which is more convenient for analytical analysis. The target and CE output response dynamics in this model, $H_{o_t}(j\omega)$ and $H_{o_x}(j\omega)$, are given by:

$$H_{o_t}(j\omega) = [H_{o_f}(j\omega)H_{o_{e^\star}}(j\omega)e^{\tau_f j\omega} + H_{o_n}(j\omega)e^{\tau_n j\omega}]H_{nms}(j\omega)e^{-\tau_v j\omega}, \tag{7}$$

$$H_{o_x}(j\omega) = H_{o_{e^\star}}(j\omega)H_{nms}(j\omega)e^{-\tau_v j\omega}. \tag{8}$$

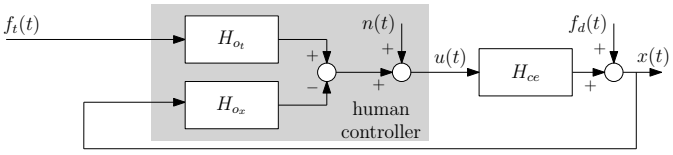

Fig. 4. Simplified control diagram of the preview model.

2.3 Perfect Target-Tracking

From Fig. 4, the closed-loop target-to-CE output dynamics in the frequency domain can be derived to be

$$\frac{X(j\omega)}{F_t(j\omega)} = \frac{H_{ce}(j\omega)H_{o_t}(j\omega)}{1 + H_{ce}(j\omega)H_{o_x}(j\omega)}. \quad (9)$$

The goal to align the CE output with the target is equivalent to adopting closed-loop dynamics equal to one. Substitution of $X(j\omega)/F_t(j\omega) = 1$ in (9) and solving for the perfect target-tracking dynamics $H^P_{o_t}(j\omega)$ yields:

$$H^P_{o_t}(j\omega) = \frac{1}{H_{ce}(j\omega)} + H_{o_x}(j\omega). \quad (10)$$

The structure of $H_{o_x}(j\omega)$ is fixed for a given CE in accordance with (8), so the perfect setting of $H_{o_t}(j\omega)$ is also fixed. For integrator CE dynamics, $1/H_{ce}$ is a differentiator and $H_{o_x}(j\omega)$ can be approximated by a gain in a large frequency range. Therefore, $H_{o_x}(j\omega)$ will dominate the perfect target-response dynamics at low frequencies, where the contribution of $1/H_{ce}$ is negligible, while the opposite is true at high frequencies. Interestingly, the structure of the modeled HC's target response in (7) is similar: at low frequencies it is dictated by gain $K_f K_{e^\star}$ and at high frequencies by differentiator $K_n j\omega$. This suggests that HCs indeed attempt to respond to the target in a way that results in optimal performance.

3. HUMAN CONTROLLER MODEL FITTING

Here, we explain the parameter estimation method, applied to fit the introduced HC model to experimental measurements. Additionally, we present the calculation of the model's quality-of-fit in terms of the VAF.

3.1 Model Parameter Estimation

To estimate the model parameters, we used a frequency-domain method that minimizes the difference between the measured control inputs $U(j\omega)$ and the simulated control inputs $\hat{U}(j\omega|\Theta)$. The parameter vector Θ is $[K_n \;\; \tau_n \;\; K_f \;\; T_{l,f} \;\; \tau_f \;\; K_{e^\star} \;\; \omega_{nms} \;\; \zeta_{nms} \;\; \tau_v]$. To increase the accuracy of the estimated parameters, the cost function J only accounts for the modeling error at the 40 input frequencies ω_i of the target and disturbance signals (see Section 4.3 for details), where the signal-to-noise ratio is generally high:

$$J = \sum_{i=1}^{40} |U(j\omega_i) - \hat{U}(j\omega_i|\Theta)|^2. \quad (11)$$

Assuming zero remnant, it follows from Fig. 4 that the simulated control action can be calculated in the frequency domain as

$$\hat{U}(j\omega_i|\Theta) = H_{o_t}(j\omega_i|\Theta)F_t(j\omega_i) - H_{o_x}(j\omega_i|\Theta)X(j\omega_i). \quad (12)$$

The optimal parameter set is found by minimizing (11), using a Nelder-Mead simplex algorithm (Lagarias et al., 1998) with 100 random initializations.

3.2 Variance Accounted For

The VAF is a measure for the similarity between two signals. When applied to compare the modeled and the measured control inputs, it inherently serves as a measure for the ability of the model to replicate the measured HC behavior. The VAF can be estimated by

$$\text{VAF} = \left(1 - \frac{\sum_{k=1}^{N_s} P_{\epsilon_u \epsilon_u}(k\omega_b)}{\sum_{k=1}^{N_s} P_{uu}(k\omega_b)} \right) \times 100\%, \quad (13)$$

with P the estimated periodogram of the respective subscripted signals, N_s the number of samples in the measured time-traces, and ω_b the measurement's base frequency. ϵ_u is the modeling error, or the difference between the measured and simulated control signals; it is calculated as

$$E_u(j\omega) = U(j\omega) - \hat{U}(j\omega|\Theta), \quad (14)$$

with $\hat{U}(j\omega|\Theta)$ according to (12). The maximum value of the VAF is 100%, indicating that two signals are identical.

4. THE EXPERIMENT

4.1 Experiment and Apparatus

A combined target-tracking and disturbance-rejection task (see Fig. 2) was performed in the fixed-base, part-task simulator at the Faculty of Aerospace Engineering, Delft University of Technology. The experimental set-up is pictured in Fig. 5; however, the experiment was performed with low ambient light, so the preview display (layout as in Fig. 1) was clearly visible. It was presented with bright green lines on the black screen, measuring 36 by 29.5 cm, and 1280 by 1024 pixels, and it was approximately 80 cm from the subjects eyes. The side-stick used to generate control inputs could only move around its roll axis and was restrained in all other directions. It was electro-hydraulic servo-controlled and had a moment arm of 9 cm. Its torsional stiffness and damping were set to 3.58 Nm/rad and 0.20 Nm·s/rad, respectively, its mass moment of inertia to 0.01 kg·m^2, and its gain to 0.175 inch/deg. The CE was an integrator with a gain of 1.5 (i.e., $H_{ce} = 1.5/s$), making this a rate control task.

4.2 Independent Variables

The experiment had one independent variable with six levels, namely displayed preview time, which was varied between 0, 0.1, 0.25, 0.5, 0.75, and 1 s. The first and last conditions were included to compare the current results

Fig. 5. Experiment setup.

with those reported in (Van der El et al., 2015). The other values were evenly distributed between these extremes with steps of 0.25 s. Previous research (Reid and Drewell, 1972; Tomizuka and Whitney, 1973; Ito and Ito, 1975) reported a rapid performance increase for very low preview times, motivating the introduction of an extra condition with 0.1 s of preview. A performance asymptote is reported above the critical preview time of 0.5 s, so we expected to capture the complete HC's behavioral adaption with this experimental design.

4.3 Forcing Functions

The target and disturbance forcing functions were constructed to be quasi-random sums of 20 sinusoids, custom in manual control experiments (McRuer et al., 1965; Damveld et al., 2010):

$$f_t(t) = \sum_{i=1}^{20} = A_t(i)\sin(\omega_b k_t(i)t + \phi_t(i)),$$
$$f_d(t) = \sum_{i=1}^{20} = A_d(i)\sin(\omega_b k_d(i)t + \phi_d(i)). \qquad (15)$$

The i^{th} sinusoid has amplitude $A(i)$, phase $\phi(i)$, and frequency $\omega_b k(i)$. To avoid spectral leakage, each sinusoid exactly fits the measurement time of 120 s, hence their frequencies are integer multiples $k(i)$ of the base frequency ω_b. This forcing function design ensures high signal-to-noise ratios at the input frequencies, resulting in accurate estimates of the model parameters. The input frequencies were distributed between approximately 0.1 and 16 rad/s.

The used forcing functions are identical to those used in (Van der El et al., 2015), hence the target and disturbance signal standard deviations are 0.5 and 0.2 inch, respectively. They had a square spectrum with a bandwidth of approximately 1.5 rad/s, augmented with a high frequency shelf, whose amplitudes were attenuated by a factor of about 4 (target) and 3 (disturbance). We used five different realizations of the target, to preserve its unpredictable nature after repeated exposure during the experiment. As no preview is present on the disturbance, such precautions were unnecessary for this forcing function and only a single realization was used. For details on the forcing functions' frequencies, amplitudes and phases see (Van der El et al., 2015).

4.4 Participants and Experimental Procedures

Six male volunteers participated in the experiment. They were instructed to minimize the tracking error, using a strategy that they thought was best. Each subject was presented with all six conditions in a randomized order, according to a balanced latin-square design.

First, subjects were given the opportunity to familiarize themselves with the experiment by performing each condition at least once. After this the actual measurements started. A condition was trained until the experimenter observed that tracking performance stabilized. Then, the measurements were collected from five consecutive runs, after which the subjects moved on to the next condition. After each run, the root-mean-square of the tracking error signal was reported to the participants as an indication of their performance. They were challenged to keep improving their scores, to motivate them throughout the experiment. Breaks were scheduled after each block of two conditions to reduce possible effects of fatigue. The total experiment took three hours per subject, on average.

A run-in time of 8 s was added at the beginning of the 120 s runs to eliminate any transients, so these data were not used in the analysis. The time traces of the error $e(t)$, CE output $x(t)$, and operator control output $u(t)$ were sampled at 100 Hz during the experiment.

4.5 Dependent Variables

The variance of the error (σ_e^2) was used as measure for the attained tracking performance. It was calculated in the frequency domain, so we could identify the individual contributions of the target, disturbance and remnant frequencies. The fitted model served as a (parametric) measure for the subjects' control behavior. It was fitted to the frequency-domain average of the measured time signals over the five runs. The obtained HC dynamics, $H_{o_t}(j\omega)$ and $H_{o_x}(j\omega)$, and two of the model parameters, τ_n and τ_f, were analyzed to learn how HCs use the displayed preview information for control. The model VAF served as a measure for the model's validity, it was also calculated based on frequency-domain average of the measured time signals over the five runs. 95% confidence intervals were all corrected for between-subject variability.

4.6 Hypotheses

With the experiment, we tested the following hypotheses:

- I: Tracking performance will improve with increasing preview, but only up to 0.5 s, after which it stabilizes (Reid and Drewell, 1972; Ito and Ito, 1975);
- II: Conditions with more preview yield HC target response dynamics $H_{o_t}(j\omega)$ that better resemble those required for perfect target-tracking (defined by (10));
- III: In conditions with more preview, better performance is achieved by adopting near- and far-points that are farther ahead (higher τ_n and τ_f), to acquire more phase lead.

5. RESULTS

5.1 Tracking Performance

Fig. 6 shows that tracking performance improves considerably with increasing preview time (characterized by a

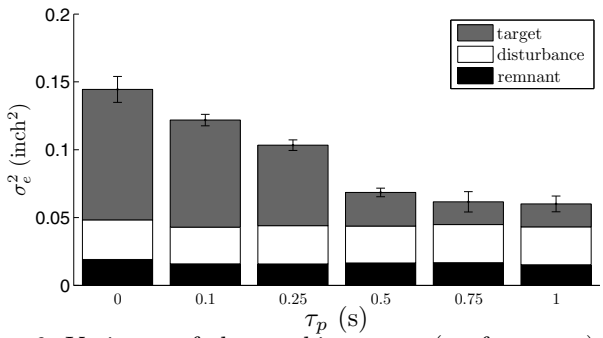

Fig. 6. Variance of the tracking error (performance), errorbars indicate the 95% confidence interval.

lower σ_e^2). Performance indeed stabilizes for preview times above 0.5 s, which corresponds well with previous findings (Reid and Drewell, 1972; Ito and Ito, 1975). The performance increase is achieved mainly at the target input frequencies (gray portions of the bars); differences at the disturbance and remnant frequencies are small.

5.2 Human Controller Dynamics

As a representative example, the estimated dynamics for Subject 1 are shown in Fig. 7. With longer preview times the magnitude of $H_{o_x}(j\omega)$ becomes slightly lower (Fig. 7 top right), but this effect is small and not consistent over subjects. Because the differences are small, the theoretically perfect target response $H_{o_t}^P(j\omega)$ is approximately equal regardless of the preview time, according to (10). $H_{o_t}^P(j\omega)$ is drawn with a solid black line in Fig. 7, based on the measured $H_{o_x}(j\omega)$ for the condition with 1 s of preview.

Fig. 7 (bottom left) shows that subjects indeed generate more phase lead in their target response when the preview time increases. With more preview, the phase characteristics better resemble those of $H_{o_t}^P(j\omega)$, which corresponds to the found performance improvement (Fig. 6). Especially the 0.75 and 1 s preview conditions, up to frequencies of about 8 rad/s, have phase characteristics similar to those of the perfect response. In these two conditions the measured performance was also similar, suggesting this is the best possible control strategy and the highest achievable performance, even with unrestricted preview

For Subject 1, the magnitude of the target response remains roughly equal, regardless of the preview time. Substantial between-subject variability is found though, specifically in conditions with 0.75 and 1 s of preview and at high frequencies. Van der El et al. (2015) suggested that a magnitude drop appears at high frequencies when a subjects ignores the target's high frequencies, and that a magnitude peak appears when subjects respond to these using a near-point.

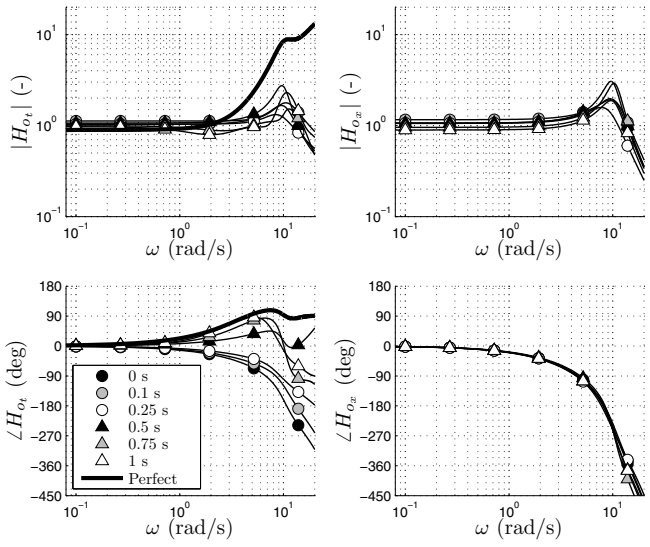

Fig. 7. Estimated HC dynamics, Subject 1. The markers only meaning is to distinguish between conditions.

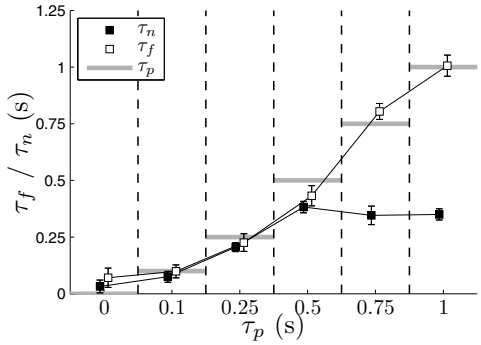

Fig. 8. Near- and far-point negative delays, means and 95% confidence intervals.

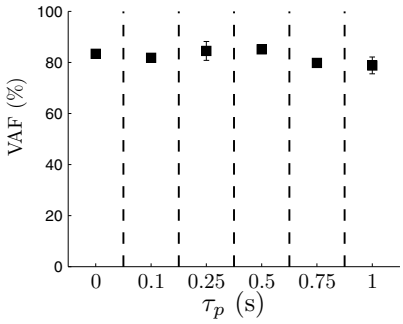

Fig. 9. Model VAFs.

5.3 Near- and Far-Point Positions

According to the model, the additional phase lead in the target response is caused by HCs responding to the target ahead. The estimated positions of the points responded to are given by the negative delays τ_n and τ_f in Fig. 8. Indeed, τ_n and τ_f increase with displayed preview time, which is in accordance with the increased phase lead (see Fig. 7).

For lower preview times, up to 0.5 s, τ_n and τ_f are identical, indicating that subjects responded to a single point on the target ahead. In conditions with 0.75 and 1 s preview, the near- and far-point positions clearly separate. The near point stabilizes at 0.35 s ahead, effectively compensating for the subjects' response delay τ_v (≈ 0.32 s, not shown). The far point continues to move farther ahead, remaining on the limit of the presented preview.

Although we estimated the parameters without bounds, both τ_n and τ_f are generally lower than the preview time τ_p (see Fig. 8). This strengthens the model's physical foundation, as it shows that subjects responded to a part of the previewed target ahead that is explicitly visible. The nonzero values found for the zero preview (pursuit) condition result from fitting the full preview model to the data, which contains more parameters than strictly needed to describe HC behavior in pursuit tracking tasks (Van der El et al., 2015).

5.4 Variance Accounted For

The calculated model VAFs are shown in Fig. 9. The means are well above 80% in all conditions, indicating that much of the measured control behavior is captured by the model. These values are similar to those often found in

compensatory manual control studies, like (Damveld et al., 2010).

6. DISCUSSION

A human-in-the-loop experiment was performed to investigate the effect of preview time on manual control behavior. Similar to previous studies (Reid and Drewell, 1972; Ito and Ito, 1975), we found that tracking performance increases substantially with the introduction of preview, and that the critical preview time is between 0.5 and 0.75 s. This confirms our first hypothesis.

By analyzing the results with a new HC model for preview tracking tasks, we gained a deeper insight in the control mechanisms that cause this performance increase. With more preview, the phase of the HC's target response better resembles that required for perfect target-tracking. However, the magnitude does not consistently improve, so our second hypothesis is only partially confirmed. The additional phase lead with higher preview time corresponds to increasingly large look-ahead times τ_n and τ_f. By responding to the target ahead HCs effectively introduce negative time delays into the system, which compensates for their response lags and the CE's inherent lag. This confirms our third hypothesis.

A transition in control behavior was found when the preview time increases from 0.5 to 0.75 s. For preview times below 0.5 s, the near- and far-point are identical, but they separate with more preview, such that two distinctly different, parallel responses are initiated. HCs position the near-point such that they approximately compensate for their response delay, while the far point is always positioned at the far limit of the displayed preview. However, for preview times beyond 1 s the far point will likely stabilize around this point; because the target response phase characteristics are nearly perfect, a higher τ_f will be of marginal benefit, if any.

The critical preview time is known to depend, at least, on the CE dynamics (Ito and Ito, 1975; Tomizuka and Whitney, 1973). Because it is not known if HCs adapt to the preview time similarly in all tasks, we plan further experiments with other CEs. Nonetheless, this paper proved the value of the new HC model for preview tracking tasks from (Van der El et al., 2015), which yielded insights about HC behavior that have not been matched before. Moreover, our experimental results further extend the model's validity, which is promising considering possible extensions to practical control tasks with preview, like driving.

7. CONCLUSION

In this paper, the effect of preview time on human control behavior was investigated. The results of a tracking experiment with integrator dynamics confirmed previous findings that tracking performance increases substantially with the first 0.5 s of preview that is displayed. Additional preview beyond 0.75 s yields no further performance benefit. A recently derived, quasi-linear human controller model accurately captures the measured behavior in all conditions, with preview times ranging from 0 to 1 s. The human's response to the target signal resembles the dynamics required for "perfect target-tracking" increasingly better when more preview is available, especially in phase. Human controllers respond to a point at the far limit of the previewed target trajectory when up to 1 s of preview is shown. They initiate an additional parallel response with respect to a nearer point when the preview time is larger than 0.5 s.

REFERENCES

Damveld, H.J., Beerens, G.C., van Paassen, M.M., and Mulder, M. (2010). Design of Forcing Functions for the Identification of Human Control Behavior. *Journal of Guidance, Control, and Dynamics*, 33(4), 1064–1081.

Ito, K. and Ito, M. (1975). Tracking Behavior of Human Operators in Preview Control Systems. *Electrical Engineering in Japan*, 95(1), 120–127. (Transl,: D.K. Ronbunshi, Vol. 95C, No. 2, Feb. 1975, pp 30-36).

Kondo, M. and Ajimine, A. (1968). Driver's Sight Point and Dynamics of the Driver-Vehicle-System Related to It. In *Proceedings of the SAE Automotive Engineering Congress*. Detroit, MI.

Lagarias, J.C., Reeds, J.A., Wright, M.H., and Wright, P.E. (1998). Convergence Properties of the Nelder-Mead Simplex Method in Low Dimensions. *SIAM Journal of Optimization*, 9(1), 112–147.

McRuer, D.T., Graham, D., Krendel, E.S., and Reisener, W.J. (1965). Human Pilot Dynamics in Compensatory Systems, Theory Models and Experiments with Controlled Element and Forcing Function Variations. Technical Report AFFDL-TR-65-15, Air Force Flight Dynamics Laboratory, Wright-Patterson Air Force Base, OH.

Mulder, M. and Mulder, J.A. (2005). Cybernetic Analysis of Perspective Flight-Path Display Dimensions. *Journal of Guidance, Control, and Dynamics*, 28(3), 398–411.

Poulton, E.C. (1974). *Tracking Skills and Manual Control*, 187–189. Academic Press, New York, NY.

Reid, L.D. and Drewell, N.H. (1972). A Pilot Model for Tracking with Preview. In *Proceedings of the 8th Annual Conference on Manual Control*, 191–204. Ann Arbor, MI.

Sheridan, T.B. (1966). Three Models of Preview Control. *IEEE Transactions on Human Factors in Electronics*, 7(2), 91–102.

Tomizuka, M. and Whitney, D.E. (1973). The Preview Control Problem with Application to Man-Machine System Analysis. In *Proceedings of the 9th Annual Conference Manual Control*, 429–441. Cambridge, MA.

Van der El, K., Pool, D.M., Damveld, H.J., Van Paassen, M.M., and Mulder, M. (2015). An Empirical Human Controller Model for Preview Tracking Tasks. *IEEE Transactions on Cybernetics*, accepted for publication.

Van Lunteren, A. (1979). *Identification of Human Operator Describing Function Models with One or Two Inputs in Closed Loop Systems*. Ph.D. thesis, Mechanical Engineering, TU Delft, Delft, The Netherlands.

Wasicko, R.J., McRuer, D.T., and Magdaleno, R.E. (1966). Human Pilot Dynamic Response in Single-loop Systems with Compensatory and Pursuit Displays. Technical Report AFFDL-TR-66-137, Air Force Flight Dynamics Laboratory, Wright-Patterson Air Force Base, OH.